Effects of Cooling on the SNR and Contrast Detection of a Low-Light Event-Based Camera

Xavier Berthelon, Guillaume Chenegros, Thomas Finateu, Sio-Hoi Ieng, and Ryad Benosman

***Abstract*—Johnson–Nyquist noise is the electronic noise generated by the thermal agitation of charge carriers, which increases when the sensor overheats. Current high-speed cameras used in low-light conditions are often cooled down to reduce thermal noise and increase their signal to noise ratio. These sensors, however, record hundreds of frames per second, which takes time, requires energy, and heavy computing power due to the substantial data load. Event-based sensors benefit from a high temporal resolution and record the information in a sparse manner. Based on an asynchronous time-based image sensor, we developed another version of this event-based camera whose pixels were designed for low-light applications and added a Peltier-effect-based cooling system at the back of the sensor in order to reduce thermal noise. We show the benefits from thermal noise reduction and study the improvement of the signal to noise ratio in the estimation of event-based normal flow norm and angle and particle tracking in microscopy.**

***Index Terms*—Event-based, low-light, neuromorphic, optical flow, Peltier-effect.**

I. Introduction

NEUROMORPHIC vision sensors have recently gained popularity in computer vision. They are built on a biomimetic approach and acquire information in a sparse manner. Unlike their frame based counterparts, which are governed by a synchronous time clock, they do not record a stack of images. Instead, asynchronous cameras are composed of an array of fully independent pixels which generate a signal only when a significant illuminance change occurs at the pixel level. In other words, a pixel that is not stimulated produces no data while a pixel that detects intensity changes sends the information with a high temporal resolution, down to the microsecond. No redundant information from the static background is recorded thus enabling ultra-fast computing on the time varying signal [1], [2]. This technology has led to the development of a first dynamic vision sensor (DVS) sensitive only to the spatiotemporal changes in the scene [3]–[5]. Similarly, an asychronous time-based image sensor (ATIS) [6], [7] was designed with the ability to record both a change detection and an exposure measurement at the pixel level with a high temporal precision. Those cameras were initially designed to acquire data in a bright outdoor environnement. They have a large dynamic range of 120 dB which enables the observation of both daylight scenes and bright objects. However they still have thermal noise which results in random pixels triggering an event despite no significant light change occurs in the scene. We designed, based on the ATIS, a new version of the camera called Helmtest. Its pixels are conceived to be more sensitive to the detection of low contrast variations under low light illumination, as it is often the case, for instance, in microscopy. We added on the Helmtest camera a cooling system that relies on the Peltier effect in order to reduce thermal noise to its minimum and increase the signal to noise ratio as described in [8], [9]. To assess the performances of the cooled event-based vision sensor in the context of low light microscopy, we are focusing on two event-based algorithms that can be applied to classical microscopy imaging problems such as the estimation of blood velocity via the visual flow and the automatic counting of cells via an event-based tracker as presented in [10]. This tracker is providing similar result as in [2] but with a smaller computational cost in the case of non overlapping cells. These two problems have been widely explored in frame-based microscopy imaging:

- to characterized blood flow dynamic, also know as blood velocimetry, classical optical flow or cross correlation technique can be used [11], [12].
- automatic cells counting can be achieved by using detection techniques such as the Hough transform [2].

These techniques are designed for frame based algorithms and the objective here is not to compare these methods to their event-based counterparts, but rather to emphasize why the algorithms evaluated here can benefit from a cooling system under low light condition, such as in intravital microscopy or in Optical Coherence Tomography (OCT) imaging. It is not trivial to distinguish precisely the contribution of a higher SNR due to the cooled sensor from the limitation of each algorithm. We are rather aim at providing the raw performances of each algorithm, for similar lighting conditions, with and without cooling the sensor.

Manuscript received June 15, 2018; revised August 26, 2018 and September 25, 2018; accepted September 27, 2018. Date of publication October 17, 2018; date of current version December 31, 2018. This work was supported by the European Research Council Helmholtz under Synergy Grant 610 110. This paper was recommended by Associate Editor V. Gruev. *(Corresponding author: Xavier Berthelon.)*

X. Berthelon, G. Chenegros, and S.-H. Ieng are with the Sorbonne Universite, INSERM, CNRS, Institut de la Vision, Paris F-75012, France (e-mail: xavier.berthelon@inserm.fr; guillaume.chenegros@obspm.fr; siohoi.ieng@gmail.com).

T. Finateu is with the Prophesee, Paris 75012, France (e-mail: tfinateu@prophese.ai).

R. Benosman is with the Sorbonne Universite, INSERM, CNRS, Institut de la Vision, Paris F-75012 France, with the University of Pittsburgh Medical Center, Pittsburgh PA 15213-2592 USA, and also with Carnegie Mellon University, Robotics Institute, Pittsburgh PA 15213-3890 USA (e-mail: benjry.benos@gmail.com).

Color versions of one or more of the figures in this paper are available online at http://ieeexplore.ieee.org.

Digital Object Identifier 10.1109/TBCAS.2018.2875202

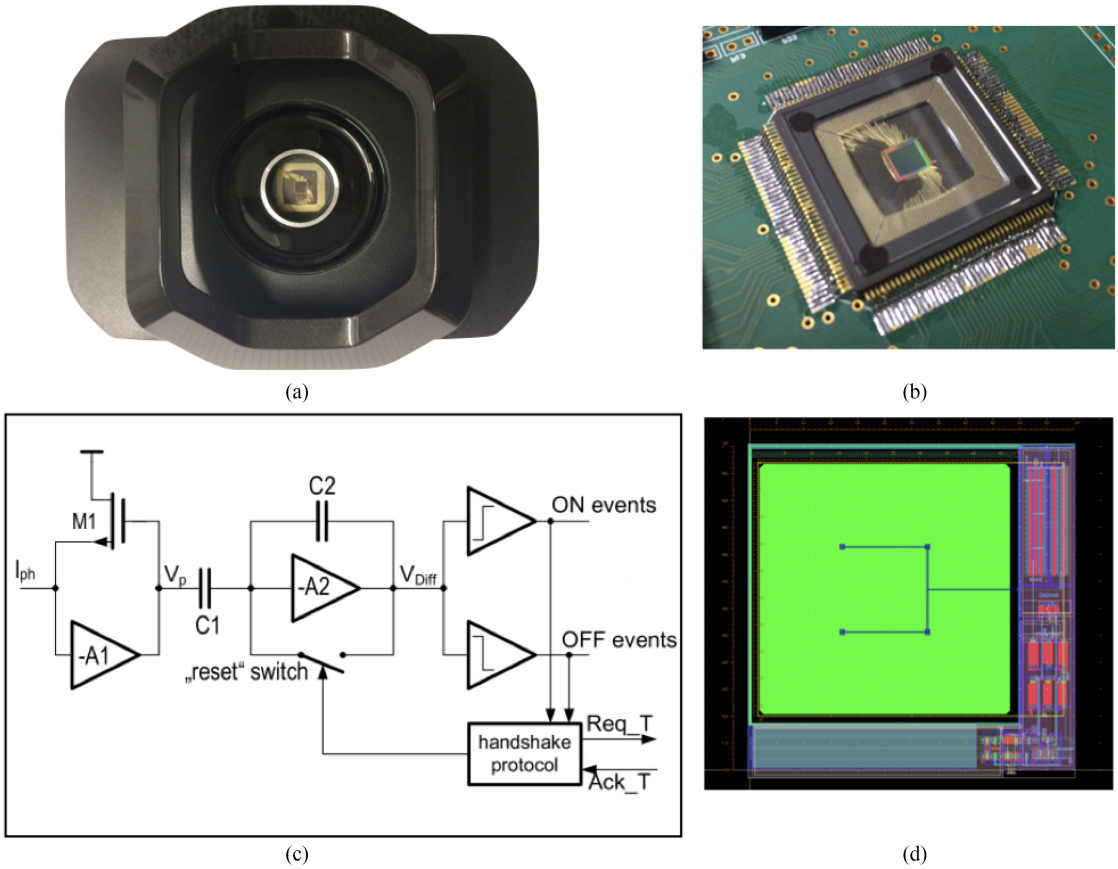

Fig. 1. (a) Helmtest camera, (b) photography of the Helmtest chip on the PCB, (c) electronic detail of the pixel, (d) layout of a single Helmtest pixel.

II. Neuromorphic Camera

The Helmtest camera shown on Fig. 1(a) is an asynchronous camera composed of a 62 $\times$ 62 array of fully independent pixels with a 60 μm pitch. The Helmtest event-based sensor is a variation of the ATIS and was designed as a collaborative work with Prophesee in order to improve the event-based sensor performances in low light condition. To achieve this, each pixel has a fill factor of 60% (as opposed to the 11% of the ATIS). Fig. 1(b) is showing the physical chip designed by Prophesee and the circuit designed is shown in 1(c). In 1(d) the layout of a single pixel is shown.

On each pixel is embedded a fast continuous logarithmic photo-receptor with asynchronous event-driven signal processing similar to what is done in the ATIS design. A change of illuminance results in a change of the photo-current. This photo-current I_{ph} is continuously monitored and sent to two voltage comparators which generate ON and OFF events when there is a significant increase or decrease in the photo-current Fig. 1(c).

As soon as the variations of the log illuminance at the pixel level is greater than a fixed threshold n, the change detector unit sends an event with a given (x, y) address, a microsecond accurate timestamp and a polarity equal to ± 1 depending on the positive or negative variation of the intensity as shown on Fig. 2. The camera's internal electrical components are tuned via a set of analogical values called "bias". For each experiment these

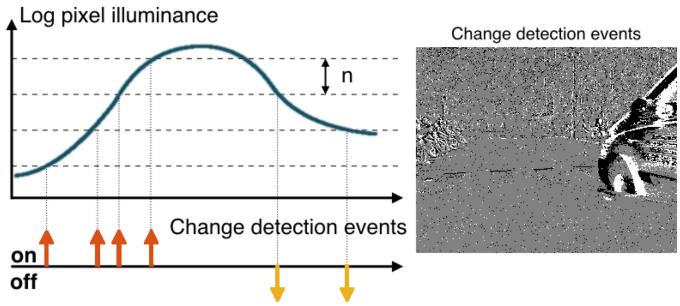

Fig. 2. Working principle of the Helmtest camera: relative changes of illuminance greater than a threshold n produce ON/OFF events depending on a positive/negative change of contrast.

"bias" are optimized depending on the illuminance and are not modified when changing the temperature of the sensor.

III. Experimental Methods

We use, for the characterization of the sensor, a modular integrating sphere from Thorlabs [14] which ensures a uniform light pattern on each pixel of the camera. The homogeneity of the output light is guaranteed at 2% and the light power is monitored using a Thorlabs power-meter. The light source used is a warm white 570 mW LED which spectrum ranges from 400 nm to 800 nm.

Low light conditions are often encountered in microscopy, which is the reason why we developed this sensor. We use for the characterization of the camera two different illuminances:

- A *low illumination* of 2 lux.
- A *higher illumination* of 10 lux.

These two illuminances are the lowest values at the sensor plan in respectively reflection and transmission microscopy that we measured on our setups.

We ensure that the sensor is well illuminated and at a fixed distance from the integrating sphere. The LED is supplied with DC current in order to avoid any blinking artifact and its power is controlled with an external generator that sends rectangular type signals at a frequency of 200 Hz. In this respect, we can precisely control the time variations of the illuminance.

We study here the event-probability after a homogeneous brightness change. The event probability $P(evt)$ is defined as the ratio between the number of times a pixel was triggered during a set of simulations $N_{trigger}$ and the number of simulations N_{simu}:

$$P(evt) = \frac{N_{trigger}}{N_{simu}} \tag{1}$$

The probability shown in Eq. (1) is established both for the ON and the OFF events because of physical differences in the electronic implementing of the ON and OFF comparators. However the characterization process provides similar probabilities for both polarities. For this reason we are only working with the ON events to limit computations.

Some pixels, commonly called "hot pixels", generate more events than they should for instance when they are defective. In this case, the probability is often much higher than 1. The frequency at which the change of illuminance occurs is 200 Hz therefore the frequency of the polarity inversion in a stream of events for one pixel should not exceed this value (ON events for the increase of illuminance followed by OFF events). In practice, due to noise, this value may exceed this upper limit. However we assume that the pixels which record inversions of polarity more than twice the upper limit over time are defective. Those faulty units will be discarded for this study.

We define the contrast variation Θ as the % of illuminance change with respect to an initial background. In other words:

$$\Theta = \frac{|I_2 - I_1|}{I_1} \tag{2}$$

with I_1 the background illuminance and I_2 the illuminance after the change of contrast. Again, this contrast ranges between 0 when the light level remains the same to 1 when the scene is completely dark or when the new illuminance is twice as bright (maximum value in this study). For the ATIS camera, the event probability vs. contrast variation has been measured by *Posch et al.* in [15], for different illuminances including 2 lux and 10 lux.

In this study, we set the detection threshold n previously introduced in Section II to its minimum value in order to detect the smallest contrast variations possible. The value of n enables the detection of contrast variations down to 10%. Any further reduction of this threshold results experimentally in an massive increase of the noise and a complete loss of the signal no matter if the cooling system is on or off. This is due to the physical parameters of the electronics used in the sensor.

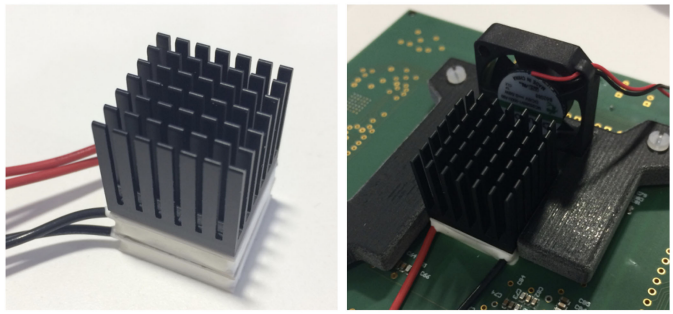

Fig. 3. On the left is a stack of 2 Peltier coolers mounted with a radiator in order to maximize heat dissipation. On the right is the system mounted on the PCB with a small fan to force convection.

Plotting the event probability vs. contrast variation would result in an ideal noise free world in a step function: 0% to 100% with an infinite slope when the minimum detection threshold is reached. It turns out that the real data are described by an "S-shaped" curve due to noise. The steeper is the slope, the closer it is to a noise free acquisition. As shown in [15], the slope of the event probability curve decreases with the background light level. In other words, when reaching low light levels, the recordings are more noise polluted. We will investigate now how we can reduce this noise when recording variations of contrast by using the Helmtest camera and a Peltier based cooling system.

IV. Performances of the Cooling System

We now look at the effect of the cooling system on the pixels' responses. A stack of Peltier coolers [16], as seen on Fig. 3, together with a fan for convection are added directly at the back of the sensor in order to reduce thermal noise. A high temperature at the sensor plan results in an increase of the thermal agitation of charge carriers. As a result, the electrons within the photo-diode are more likely to cross the energy barrier without the help of any energy from the photons. These electrons are responsible for the noise events. A reduction of the temperature forces electrons to cross their energy barrier only when a sufficient amount of energy from the photons is transmitted.

The temperature difference generated by the Peltier effect can be mathematically determined. Yet other phenomenon such as Joule heating or thermal gradient may influence the absolute value on the cold or hot side. In order to be accurate, we will measure for our experiments the temperature with a probe located at the junction between the sensor and the Peltier.

First, we investigate if there is an optimal cooling temperature, which is characterized by the following points:

- An improvement of the signal to noise ratio thanks to the reduction of thermal noise.
- The absence of condensation on our device when it is cooled down.

Condensation forms when the temperature drops and microscopic water droplets cluster. The critical temperature when this

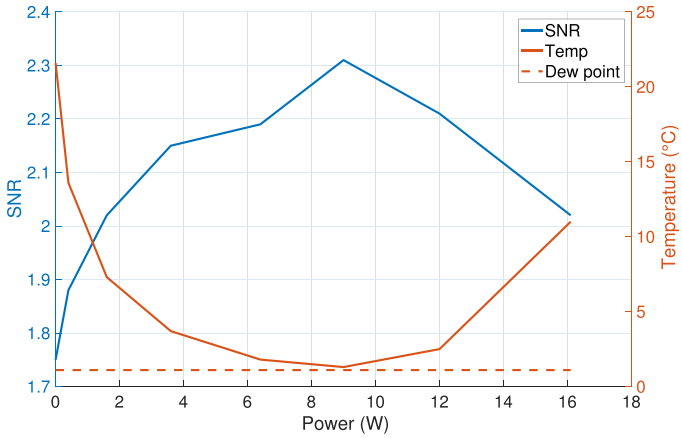

Fig. 4. In orange is the temperature at the sensor plan in Celsius, depending on the power supply in watts. The blue curve is the corresponding SNR and the orange dashed line delimits the dew point.

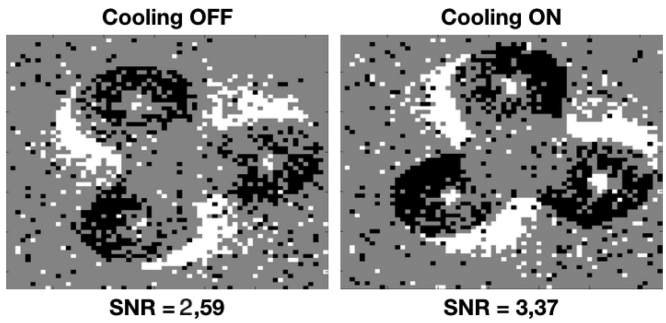

Fig. 5. Left: 20 ms recording of the fidget spinner without the cooling system. The SNR is 2.59. Right: 20 ms recording of the fidget spinner with the cooling system. The SNR is 3.37.

phenomenon occurs is called the dew point. In order to determine the dew point we need to measure the relative humidity around the sensor. We use a psychrometer system where two thermometers (dry and wet) measure the room temperature. The disparity between the temperatures measured gives an estimate of the relative humidity. Here, the temperature with the dry thermometer is 20.1° while it is 10.4° with its wet counterpart. From a standard psychrometric chart, this indicates a relative humidity of 28% [19]. We now compute the dew point temperature T_r as follow:

$$T_r = \frac{b\alpha(T, R_H)}{a - \alpha(T, R_H)} \tag{3}$$

with $b = 237,7°$, $a = 17,27°$ and α a function of the room temperature T and the relative humidity R_H defined by:

$$\alpha(T, R_H) = \frac{aT}{b+T} + ln(R_H) \tag{4}$$

The dew point is 1.1° which sets the limit for the cooling system beyond which condensation will start to appear on the sensor. Let's now measure the signal to noise ratio (SNR) value for a range of power supply from 0W to 16 W. We define the SNR as the ratio between the number of evt/μs of the global signal N_{signal} divided by the noise level N_{noise},

$$SNR = \frac{N_{signal}}{N_{noise}} \tag{5}$$

The noise level N_{noise} is the number of events generated each micro-second without any signal, in other words without light variations, in the scene. We first measure this noise under a 2lux illumination and then observe a fast rotating fidget spinner under the same light conditions. The rotation speed of the fidget spinner is externally set by a motor in order to be identical during each experiment and the temperature at the back of the sensor is controlled with a probe. Between each acquisition, the current supply of the Peltier system is adjusted and we wait for the temperature to stabilize (variations below ±0.1°) before recording. On Fig. 4 are shown the values of the SNR and the sensor temperature according to the power supply.

TABLE I
EFFECT OF THE COOLING SYSTEM ON THE NUMBER OF NOISE EVENTS

	Low illuminance		Higher illuminance	
	Uncooled	Cooled	Uncooled	Cooled
evt/μs	0.18	0.125	0.082	0.058
Std	8%	9%	9%	12%

We see that the temperature decreases with the power supply up to 9 W after which it rises again. At this point, the system reaches its heat dissipation limits. The hot side of the Peltier coolers prevents a further reduction of the local temperature. As expected the SNR is maximum right before we reached the dew point due to the reduction of thermal noise. We will therefore cool down the sensor to 1.5° when performing experiments with the cooling system.

At this temperature, the noise level of the fidget spinner recording is 0.57 evt/μs while it is 0.87 evt/μs when the cooling system is off. We therefore have a 30% attenuation of the noise level. With the activation of the Peltier coolers, the SNR was raised by a factor of 1.3 as shown on Fig. 5.

Let us now focus on the effect of the cooling system on noise reduction alone for different levels of illuminance. On Table I we see the results for both a low (2lux) and higher (10lux) illuminance. In both cases N_{noise} drops by 30% with the activation of the Peltier coolers.

In an other experiment we investigate the effect of cooling the sensor on signal detection for a set of contrast variations. As previously done, we study the event probability for the Helmtest camera under a low and higher illuminations with variations of contrast ranging from 0% to 50%. The results are displayed on Fig. 6 and Fig. 7 with a smoothing spline fitting curve model.

The red data represent the response without cooling and the blue data the response to the same stimulation with a cooling of the sensor at 1.5°. Without the cooling system we see that the "S-shaped" curves have a slight slope meaning that the recordings are noise polluted. When the sensor is cooled down, the event probability is raised and the detection function becomes closer to a step function. In both cases the steepness of the slope (computed for a 50% event probability) has been raised by 25%, hence we gain in detection sensitivity by cooling the sensor.

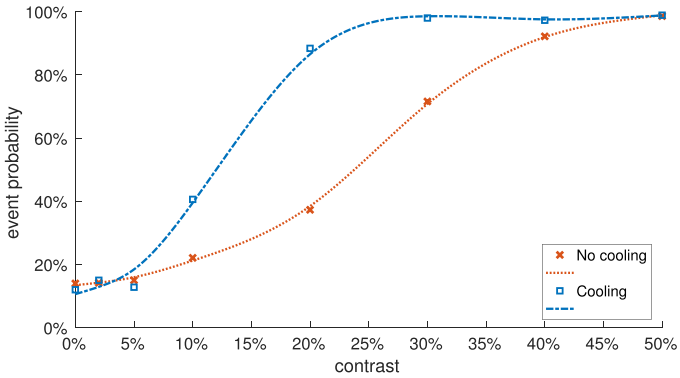

Fig. 6. Event probability vs. stimulus contrast for a low illuminance. The red curve is the result without cooling and the blue curve is the response to the same stimulation with the cooling system.

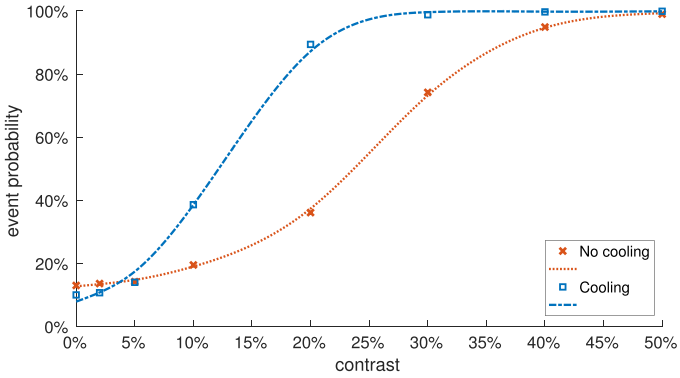

Fig. 7. Event probability vs. stimulus contrast for a higher illuminance. The red curve is the result without cooling and the blue curve is the response to the same stimulation with the cooling system.

V. Experimental Results

We now test the effect of the cooling system on a practical application of normal flow computation. Normal flow is often used in microscopy to estimate the speed of microparticles at the cellular level [17][18]. We record for this experiment a rotating fan, shown on Fig. 8, and compute the normal flow angle and norm as in [13] at the upper edge of the blade under an illuminance of 2 lux. On Fig. 9 is the normal flow computed at 275 rotations per minute (RPM) with the cooling system on and off. The color of the flow represents the value of the vector's angle: from dark blue for 0 degrees to yellow, 360 degrees. At first glance we clearly see that the normal flow seems less disrupted and more complete on the recording with the cooling system on.

We now measure both the norm and angle of the normal flow at the upper edge of the blade for a range of 275 RPM to 1730 RPM. Results are shown on Fig. 10 and Fig. 11. The yellow data correspond to the reference value for the norm and angle of the normal flow. As we know the rotation speed of the fan and its radius we estimated ground-truth mathematically. The dark red data correspond to the recordings without the cooling system and the dark blue data with the cooling system activated. Beyond 625 RPM and without the cooling system, the SNR is too weak and the signal is completely drowned in noise.

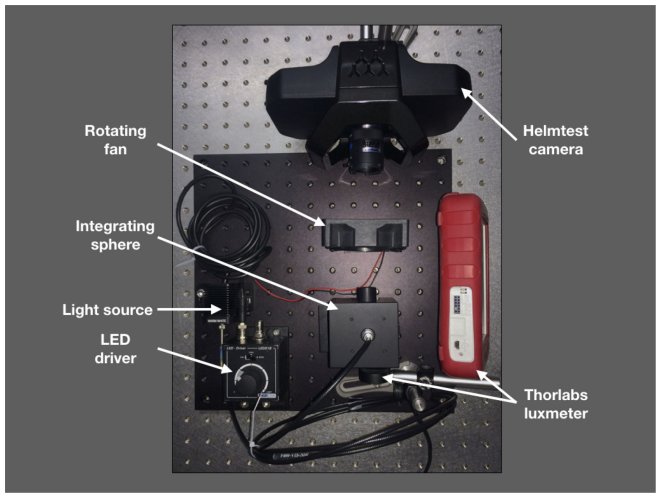

Fig. 8. Setup used to compute the normal flow on a rotating fan under a low illumination. The output of the integrating sphere is monitored with a Thorlabs power-meter.

Moreover, unlike for the angle value, the norm of the normal flow is underestimated when no cooling is activated.

Once the Peltier coolers are on, the SNR increases and the measure of the normal flow is improved. Above 1730 RPM the norm of the normal flow overshoots and diverts from the ground-truth. At this rate the number of events used to compute the flow is drastically reduced and as expected we lose precision. An increase by a factor 3 is achieved in the detection sensitivity simply by cooling down the sensor.

Additional experiments show that results are consistent on other regions of the normal flow map.

Let us now look at the effect of cooling the sensor on another application geared toward microscopy. We use for that a reflection based microscope to observe small particles floating in water. A flow is induced inside a micro-fluidic chip with a syringe as shown on Fig. 12. We tune the light power to be 2 lux at the sensor plane and use an event-based blob tracking algorithm similar to the one described in [10]. Any object moving in the field of view generates a cloud of events that can be represented by a bivariate normal distribution, in other words a blob, that updates its position with each new event. Each micro-particle is assigned with a blob tracker (in green on Fig. 13), provided that enough events are generated. This enables us to track and count the number of particles $N_{particule}$ that cross the field of view. For that we increment a counter when the center of a tracker crosses a virtual line (in red on Fig. 13).

We can fine tune the parameters of the algorithm in order to associate a tracker when very few events are generated, however we become very sensitive to noise. Indeed many trackers are falsely created due to noise events and the number of actual particles is over-estimated. This limitation sets the lower boundary for the fine tuning of the algorithm. As a result, for high particle velocities and without the cooling system, no trackers are generated and we miss objects that cross the field of view. Results are shown on Table II for a slow velocity (flow of 3 ml/h), a medium velocity (flow of 9 ml/h) and a high velocity (flow of 15 ml/h).

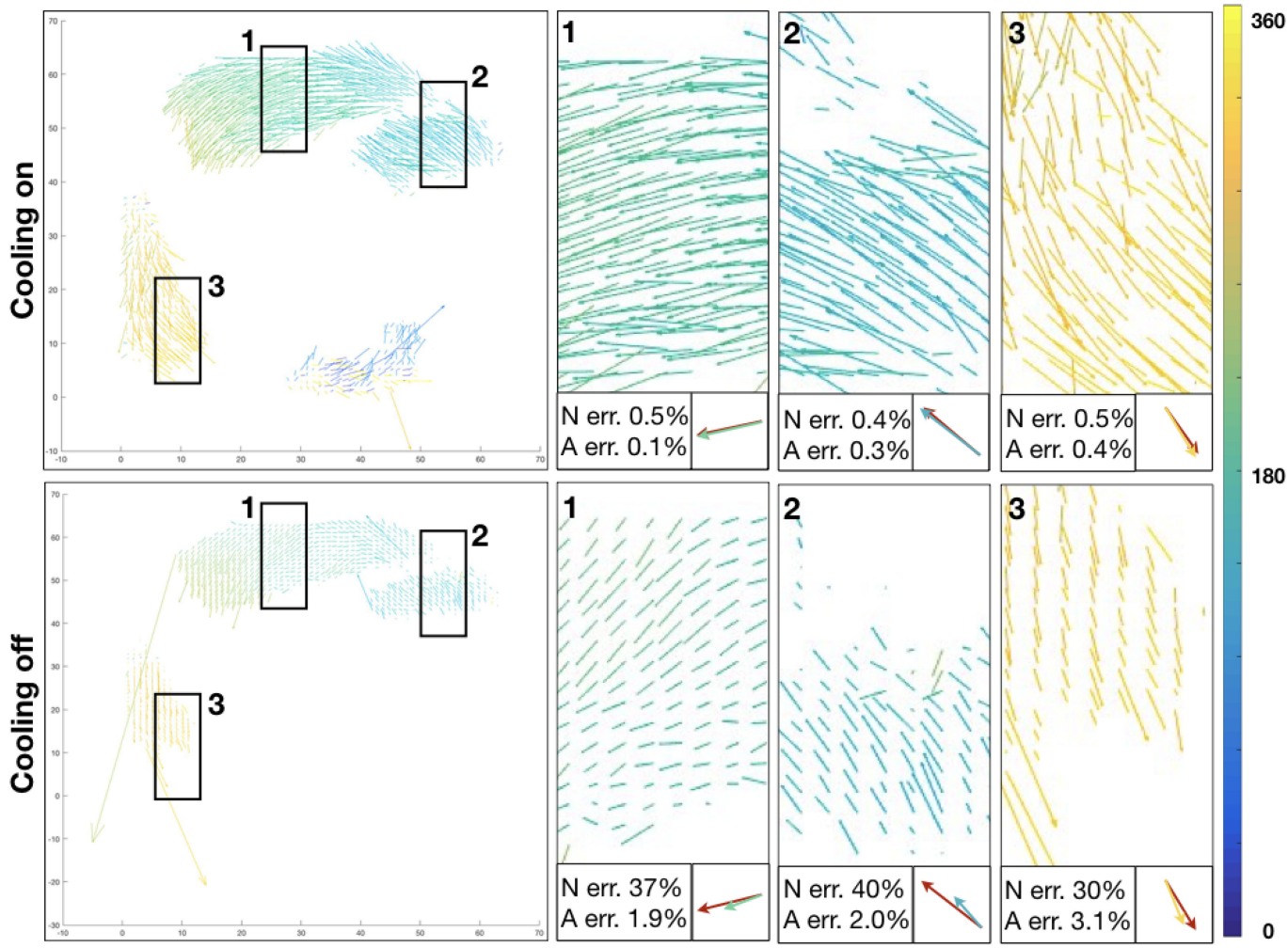

Fig. 9. Representation of the fan's normal flow at 275 RPM with both the cooling system on (top section) and off (bottom section). Areas 1, 2 and 3 are three zooms with at the bottom the mean normal flow for the widow, superimposed with the ground-truth in red. The colors correspond to the angle of the normal flow, from dark blue for 0 degrees to yellow for 360 degrees. N err. is the error of the norm from the ground-truth and A err. the error on the angle of the flow.

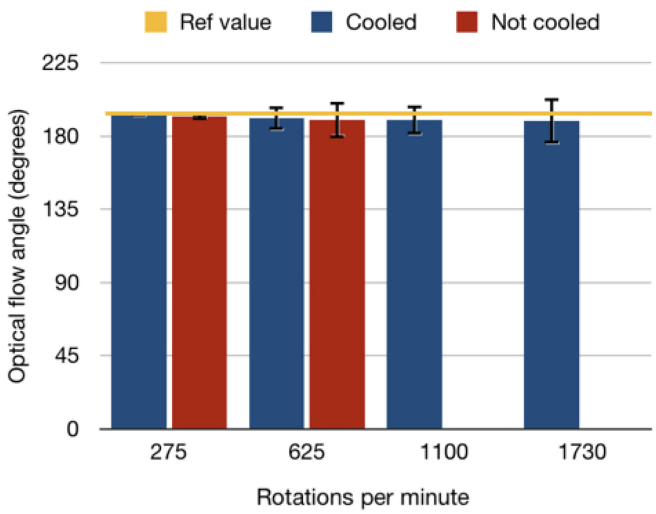

Fig. 10. Measure of the angle of the normal flow vector for different rotating speeds. The dark blue data are results with the cooling system and the dark red ones without. The yellow line corresponds to the reference value.

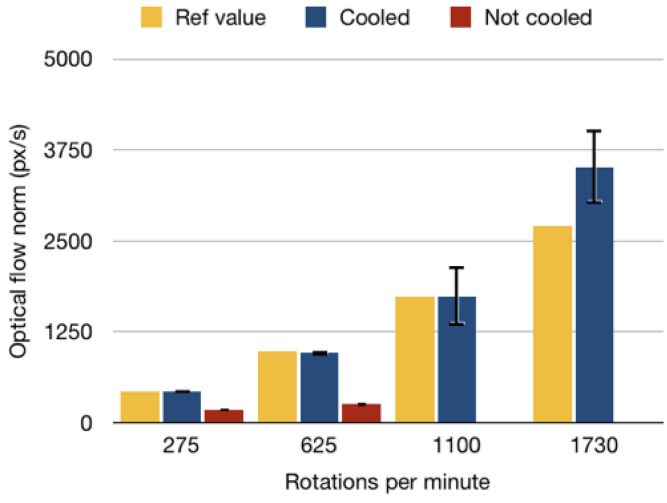

Fig. 11. Computation of the norm of the normal flow with the cooling system (dark blue) and without the cooling system (dark red). The yellow data correspond to the reference value.

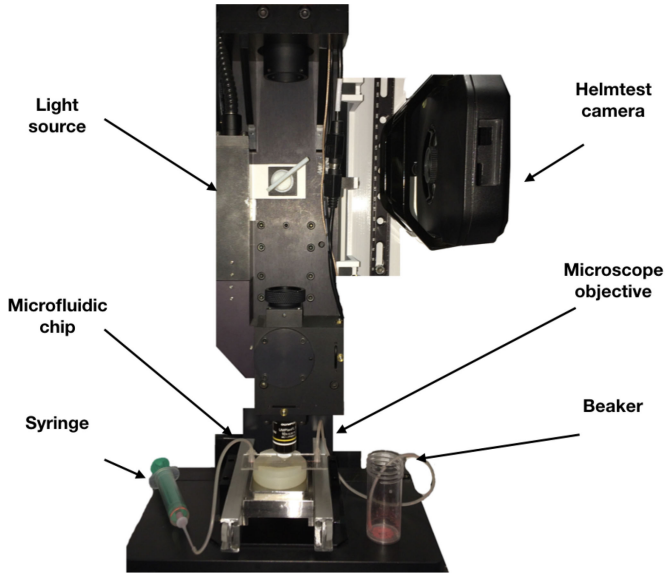

Fig. 12. Setup used to estimate the number of micro-particles crossing the field of view using a reflection based microscope, a micro-fluidic chip and a syringe.

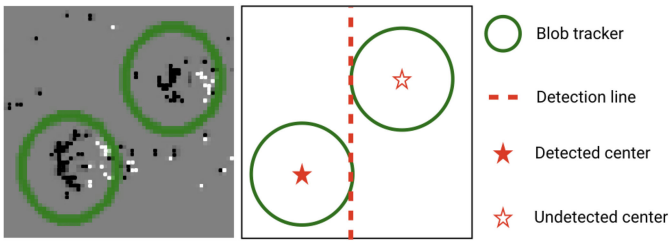

Fig. 13. Left: Illustration of the blob tracking algorithm on a frame reconstruction during 20 ms. Right: Principle of blob counting to estimate the number of particles that cross the field of view.

TABLE II
EFFECT OF THE COOLING SYSTEM ON PARTICLE COUNTING FOR DIFFERENT FLOW VELOCITIES

	Slow		Medium		Fast	
	Hot	Cold	Hot	Cold	Hot	Cold
$N_{particule}$	250	243	430	802	320	1040
Error	3%	4%	43%	8%	75%	17%

When the cooling system is activated, the noise is reduced. Particles are not generating more events but we can lower the number of minimum events to create a tracker without being noise polluted. Counting particles flowing with higher velocities is now possible. Our ground truth is obtained by manually counting the number of particles that cross the field of view.

VI. CONCLUSIONS

Asynchronous sensors have already demonstrated their potential regarding ultrafast imaging and online computation on sparse data. Despite their large bandwidth, they perform poorly in low light conditions. A bright illuminance cannot always be used in microscopy and especially in biology where side effects such as photo-bleaching must be avoided. The Helmtest event-based camera presented in this paper shows improvements compared to the ATIS camera in low light conditions and with low contrast variations. The experiment performed in microscopy shows that this device could be a potential candidate for medical imaging devices with a low light input source, like for instance reflection based microscopes. We showed with a computation of the normal flow and the tracking algorithm that cooling the sensor also significantly increases the detection and should therefore be used on any event-based sensor in order to increase the SNR.

However the full calibration of a camera would require more extensive work. Indeed, the results presented here have been obtained with a given set of parameters which were of interest for low light conditions. In particular, the camera's internal electrical components are tuned via a set of analogical values called "bias". They correspond to a list of voltage values that set the physical limits of the electronics. Depending on their values, properties of the pixels such as the detection threshold, the latency, the refractory period and many others may change. For our experiments we have been working with a fixed set of bias with the hypothesis that the camera's parameters would remain unchanged when the temperature fluctuates. In order to have a complete characterization, a measure of those parameters with and without the cooling system activated for many more light levels would be necessary.

Today, the main limitation of the Helmtest camera remains the size and number of pixels which limit the field of view and the observation of small structures. However, asynchronous sensors are improving daily. Such sensors with a VGA resolution are already available and this is only a matter of time before they can be adapted to low light conditions as well.

ACKNOWLEDGMENT

The authors would like to thank the company Silamir which designed the black casing for the Helmtest camera and its embedded cooling system.

REFERENCES

[1] D. Drazen, P. Lichtsteiner, P. Hafliger, T. Delbruck, and A. Jensen, "Towards real-time particle tracking using an event-based dynamic vision sensor," *Exp. Fluids*, vol. 51, pp. 1465–1469, 2011.

[2] Z. Ni, C. Pacoret, R. Benosman, S. Ieng, and S. Regnier, "Asynchronous event-based high speed vision for microparticle tracking," *J. Microsc.*, vol. 245, pp. 236–244, 2011.

[3] P. Lichtsteiner and T. Delbruck, "A 64X64 AER logarithmic temporal derivative silicon retina," *Res. Microelectron. Electron.*, vol. 2, pp. 202–205, 2005.

[4] P. Lichtsteiner, C. Posch, and T. Delbruck, "A 128X128 120 dB 15 s latency asynchronous temporal contrast vision sensor," *IEEE J. Solid-State Circuits*, vol. 43, no. 2, pp. 566–576, Jan. 2008.

[5] P. Lichtsteiner, C. Posch, and T. Delbruck, "A 128X128 120 dB 30 mW asynchronous vision sensor that responds to relative intensity change," in *Proc. IEEE Int. Solid-State Circuits Conf.*, 2006, vol. 51, pp. 2060–2069.

[6] C. Posch, D. Matolin, and R. Wohlgenannt, "High-DR frame-free PWM imaging with asynchronous AER intensity encoding and focal-plane temporal redundancy suppression," in *Proc. IEEE Int. Symp. Circuits Syst.*, 2010, pp. 2430–2433.

[7] C. Posch, D. Matolin, and R. Wohlgenannt, "A QVGA 143 dB dynamic range frame-free PWM image sensor with lossless pixel-level video compression and time-domain CDS," *IEEE J. Solid-State Circuits*, vol. 46, no. 1, pp. 259–275, Jan. 2011.

[8] S. B. Riffat and X. Ma, "Thermoelectrics: A review of present and potential applications," *Appl. Thermal Eng.*, vol. 23, pp. 913–935, 2003.
[9] G. Min and D. M. Rowe, "Cooling performance of integrated thermoelectric microcooler," *Solid-State Electron.*, vol. 43, pp. 923–929, 1999.
[10] X. Lagorce, C. Meyer, S. H. Ieng, D. Filliat, and R. Benosman, "Asynchronous event-based multikernel algorithm for high speed visual feature tracking," *IEEE Trans. Neural Netw. Learn. Syst.*, vol. 26, no. 8, pp. 1710–1720, Aug. 2015.
[11] K. L. Pitts and M. Fenech, "Micro particle image velocimetry for velocity profile measurement of micro blood flows," *J. Vis. Exp.*, vol. 25, no. 74, pp. 1–8, 2013.
[12] D. Guo, A. L. Van de Ven, and X. Zhou, "Tracking and measurement of the motion of blood cells using optical flow methods," *IEEE J. Biomed. Health Inf.*, vol. 18, no. 3, pp. 991–998, May 2014.
[13] R. Benosman, C. Clercq, X. Lagorce, S. Ieng, and C. Bartolozzi, "Event-based visual flow," *IEEE Trans. Neural Netw. Learn. Syst.*, vol. 25, no. 2, pp. 407–417, Feb. 2014.
[14] 2018. [Online]. Available: https://www.thorlabs.com/thorproduct.cfm?partnumber=IS200
[15] C. Posch and D. Matolin, "Sensitivity and uniformity of a 0.18 μm CMOS temporal contrast pixel array," in *Proc. IEEE Int. Symp. Circuits Syst.*, 2011, pp. 1572–1575.
[16] [Online]. Available: https://www.cui.com/product/resource/cp20.pdf
[17] X. Berthelon, G. Chenegros, N. Libert, J. A. Sahel, K. Grieve, and R. Benosman, "Full-field OCT technique for high speed event-based optical flow and particle tracking," *Opt. Express*, vol. 25, pp. 12611–12621, 2017.
[18] F. Amat, E. W. Myers, and P. J. Keller, "Fast and robust optical flow for time-lapse microscopy using super-voxels," *Bioinformatics*, vol. 29, pp. 373–380, 2013.
[19] H.-S. Ren, "Construction of a generalized psychrometric chart for different pressures," *Int. J. Mech. Eng. Educ.*, vol. 32, pp. 212–222, 2004.

Xavier Berthelon received the M.Sc. degree in optics and biomedical engineering from both the Royal Institute of Technology, Stockholm, Sweden, and from the Institut d'Optique Graduate School, Palaiseau, France. He is currently working toward the Ph.D. degree with Vision Institute, Paris, France, with the team Neuromorphic Vision and Natural Computation.

Guillaume Chenegros received the Ph.D. degree from ONERA, Palaiseau, France. He is currently an Associate Professor with the University Pierre and Marie Curie, Paris, France. He is currently a Chief Technical Officer with Chronolife, Paris, France, a startup in the field of medical monitoring. His works focuses on biomedical instrumentation and analysis of medical data.

Thomas Finateu received the M.Sc. degree from the Ecole nationale superieur d'electronique, informatique et de radiocommunications de Bordeaux, Bordeaux, France. He is currently the Head of sensor development with Prophesee, Paris, France, a company that develops neuromorphic cameras. His work covers analog RF design.

Sio-Hoi Ieng received the Ph.D. degree in computer vision from the University Pierre and Marie Curie, Paris, France, in 2005. He is currently an Associate Professor with the University Pierre and Marie Curie and a member of the Vision Institute, Paris, France. He worked on the geometric modeling of noncentral catadioptric vision sensors and their link to the caustic surface. His current research interests include computer vision, with special reference to the understanding of general vision sensors, cameras networks, neuromorphic event-driven vision, and event-based signal processing.

Ryad Benosman received the M.Sc. and Ph.D. degrees in applied mathematics and robotics from the University Pierre and Marie Curie, Paris, France, in 1994 and 1999, respectively. He is currently an Associate Professor with University Pierre and Marie Curie, leading the Natural Computation and Neuromorphic Vision Laboratory, Vision Institute, Paris, France. His work covers neuromorphic visual computation and sensing. He is currently involved with the French retina prosthetics project and with the development of retina implants, and is the Cofounder of Pixium Vision, a french prosthetics company. He is an expert in complex perception systems, which embraces the conception, design, and use of different vision sensors covering omnidirectional 360° wide-field of view cameras, variant scale sensors, and noncentral sensors. He is among the pioneers of the domain of omnidirectional vision and unusual cameras and still active in this domain. He has been involved in several national and European robotics projects, mainly in the design of artifcial visual loops and sensors. His current research interests include the understanding of the computation operated along the visual systems areas and establishing a link between computational and biological vision. He has authored more than 100 scientific publications and holds several patents in the area of vision, robotics and image sensing. In 2013, he was awarded with the national best French scientific paper by the publication La Recherche for his work on neuromorphic retinas.